Structure, formation, and motion of kinks in increasing-absorption optical bistability

M. Lindberg, S. W. Koch, and H. Haug
Institut für Theoretische Physik der Universität Frankfurt, Robert-Mayer-Strasse 8, D-6000 Frankfurt-am-Main, Federal Republic of Germany
(Received 8 July 1985)

The spatially inhomogeneous distribution of the light intensity and of the excitation density is investigated for systems showing cavityless optical bistability due to increasing absorption. The formation and motion of spatial kink structures is analyzed in detail within a rate-equation approach. Analytical estimates for the kink formation process are presented and compared to numerical results.

I. INTRODUCTION

Many semiconductor materials exhibit strong optical nonlinearities, which are interesting in themselves from a basic physics viewpoint and which, moreover, may even be used in the future for all-optical data-processing devices.[1] The physical origin of most of these dispersive or absorptive nonlinearities is the creation of electron-hole pairs which modify the optical properties. At elevated densities of electron-hole pairs, a very effective screening of the Coulomb interaction takes place, which, e.g., causes the vanishing of the exciton resonances (Mott transition). Furthermore, the single-particle energies are renormalized due to electron and hole exchange, correlation, and band-filling effects.[2]

In the present paper, we consider the case of an excitation-induced absorption. This may be caused, e.g., by the broadening of bound-exciton lines[3] or by the reduction of the semiconductor band gap due to single-particle energy renormalization by free carriers[4,5] or by thermal phonons.[6] Induced-absorption optical bistability due to these mechanisms has been observed and analyzed in some detail.[3–6] Many aspects of the phenomena are, however, quite general and occur also in other nonlinear materials.[7] In the present paper, we concentrate on the electronic band-gap reduction.

The microscopic details of our model have been described elsewhere,[4] so we only repeat the most important features. If the frequency of the exciting laser is tuned slightly below the lowest exciton resonance, one has only a weak one-photon absorption in the Urbach tail or a weak two-photon absorption in the band. Nevertheless, by these processes some electron-hole pairs are created. With increasing pair density, many-particle renormalization effects cause the band edge to shift to lower energies. At a certain density the band edge passes the laser frequency and hence, the absorption increases strongly. This increase continues until at high electron-hole-pair densities band-state filling becomes important. The absorption decreases again and vanishes when the chemical potential approaches the excitation frequency (bleaching). In Fig. 1 we plot as an example the absorption coefficient calculated for the direct-gap semiconductor CdS.[4(a)] We show the density regime for which the absorption increases, i.e., for which self-induced absorption due to band-gap reduction takes place.

When the increase of the absorption is strong enough, as in Fig. 1, there is a possibility for optical bistability. The self-induced absorptive bistability differs considerably from the usual absorptive bistability. A most important feature is that no cavity is needed. Recently, Koch *et al.*[4(b)] predicted spatial kink structures in the density profile and a corresponding sawtooth structure in the transmitted intensity when the system was excited with a pulse. Experimentally, this was confirmed by Gibbs *et al.*[6] in a sample with thermal nonlinearity. Induced-absorption bistability has been discussed as a first-order phase transition in a nonequilibrium system[8,9] and the density kinks have to be regarded in this context as a realization of two-phase spatial coexistence of regions with high and low electron-hole-pair densities.

In the present paper, we analyze theoretically both steady-state and dynamical properties of the kink structures. The results show that the dynamics of kink formation and of the almost discontinuous propagation cannot be described by steady-state properties. The sawteeth in the transmitted intensity are genuine dynamical features.

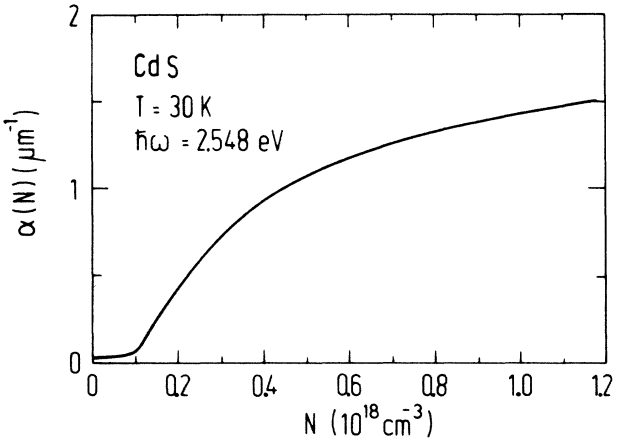

FIG. 1. Absorption coefficient α as function of the electron-hole-pair density N. Result of a microscopic calculation (Ref. 4) for CdS at a frequency below the energetically lowest exciton resonance.

In Sec. II we introduce our model and discuss its general mathematical properties. The physical results obtained are direct consequences of these properties. The stationary solutions are analyzed in Sec. III. The origin of the kink is explained and the stability of the position of the kink is studied. In Sec. IV the dynamics are investigated. Using a simple absorption model the formation of the kink is studied numerically. In a limiting case, analytic estimates are obtained and compared to the numerical results. In Sec. V we briefly summarize our results.

II. THE MODEL

We describe the properties of the system by simple rate equations.[4] The rate of change of the density of electron-hole pairs in the bulk is equal to the number of photons absorbed per unit time minus the interband spontaneous recombination rate. The simplest possible local equation is

$$\frac{\partial}{\partial t}N(z,t)=\frac{\alpha(N(z,t))}{\hbar\omega}I(z,t)-N(z,t)/\tau\ , \tag{1}$$

where α is the absorption coefficient, I the intensity, $\hbar\omega$ the energy of the photons, and τ the electron-hole-pair recombination time. If the band-gap shrinkage is caused by heating, Eq. (1) for the free-carrier density N is replaced by a corresponding equation for the temperature $T(z,t)$. This equation has the same structure; the loss term is due to transverse thermal diffusion.[6] It is possible to insert in Eq. (1) a longitudinal diffusion term.[4] In the present paper, however, we restrict ourselves to the case without diffusion. This limit is realized approximately, for example, in semiconductor microcrystallite filters.[6]

The intensity is taken to follow Beer's law. No dispersive or propagation effects are taken into account. Hence, we have

$$\frac{\partial}{\partial z}I(z,t)=-\alpha(N(z,t))I(z,t)\ . \tag{2}$$

Our goal is to describe the response of the system to pulse excitation. The pulse shape of the incident light enters as a boundary condition for $I(z,t)$ at the front end ($z=0$) of the crystal. With a pregiven pulse shape $I_0(t)$ we have

$$I(z=0,t)=I_0(t)\ . \tag{3}$$

Equation (2) can be formally integrated and we obtain

$$I(z,t)=I_0(t)\exp\left[-\int_0^z\alpha(N(z',t))dz'\right]\ . \tag{4}$$

This formula shows that in our model the intensity follows immediately the changes in the pulse shape $I_0(t)$ and in the density N. Physically it is clear that the intensity at z is not dependent on the local density but on the complete density profile in front of the position z. The fact that α is positive (no gain) manifests itself in the mathematical property that I is a monotonically decreasing function of z. An additional important property of $I(z,t)$ is that it is continuous for every $z>0$ at all times t. However, its derivative may be discontinuous.

The density N does not respond immediately to temporal changes because $\partial N/\partial t$ is finite. If the absorption is nearly constant and the input intensity varies slowly, the recombination time τ characterizes the response time of the density. In Eq. (1) z appears only parametrically. Therefore, it allows solutions for N which are discontinuous at some value of z, while the intensity $I(z,t)$ has to be continuous. When Eq. (4) is inserted into (1), we obtain the equation

$$\frac{\partial}{\partial t}N(z,t)=\frac{\alpha(N(z,t))}{\hbar\omega}I_0(t)\times\exp\left[-\int_0^z\alpha(N(z',t))dz'\right]-N(z,t)/\tau\ . \tag{5}$$

This is a nonlocal differential-integral equation for N.

Typical for the nonlinear problems is that the solutions are highly dependent on initial conditions. We use the initial condition

$$N(z,t=0)=0\ . \tag{6}$$

The increasing part of the pulse in general causes a response which is different from that caused by the decreasing part.

III. KINK STRUCTURE IN THE STEADY STATE

The existence of the kink structure obtained by Koch *et al.*[4(b)] can be qualitatively understood by studying the steady-state properties of the model. We assume that the absorption follows the general features shown in Fig. 1. In the steady state the time derivative of N is zero and we assume the input intensity to be constant. Then, the equations are

$$\frac{\alpha(N(z))}{\hbar\omega}I(z)-N(z)/\tau=0\ , \tag{7}$$

$$\frac{\partial I(z)}{\partial z}=-\alpha(N(z))I(z),\quad I(0)=I_0\ . \tag{8}$$

The density is in a local equilibrium with the local intensity. The intensity profile is determined by the density profile according to (8).

We define the critical intensities $I_\uparrow$ and $I_\downarrow$, with $I_\uparrow>I_\downarrow$, as the limiting values for which Eq. (7) has two solutions. For the absorption coefficient in Fig. 1 there are exactly two such values. Writing (7) in the form

$$\alpha(N)=\frac{\hbar\omega}{\tau}\frac{1}{I}N\ , \tag{9}$$

graphical inspection shows that the critical intensities are those for which the straight line [right-hand side of (9)] is a tangent to $\alpha(N)$ at some point (see Fig. 2). The corresponding critical densities $N_\uparrow$ and $N_\downarrow$ satisfy the equation

$$\frac{d}{dN}\left[\frac{N}{\alpha(N)}\right]=0\ . \tag{10}$$

If the input intensity is larger than $I_\uparrow$, the steady-state solution at the front face of the crystal is the solution with high absorption (upper bistable branch). The intensity decreases fast because of this high absorption. Hence, at

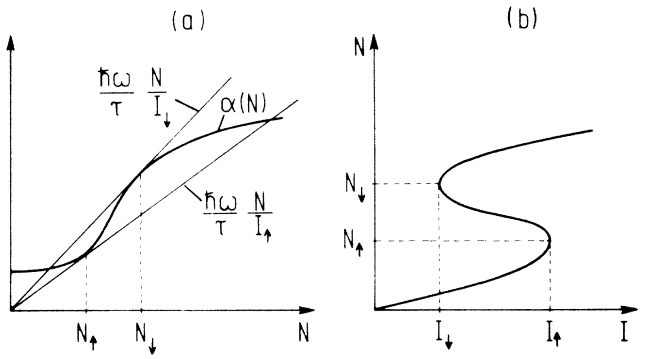

FIG. 2. (a) Geometrical solution of the stationary equation (1) (schematically). $I_\uparrow$ and $I_\downarrow$ are the critical densities for the occurrence of optical bistability, $N_\uparrow$ and $N_\downarrow$ are the corresponding density values. (b) Stationary solution for the density N as function of the intensity I (schematically).

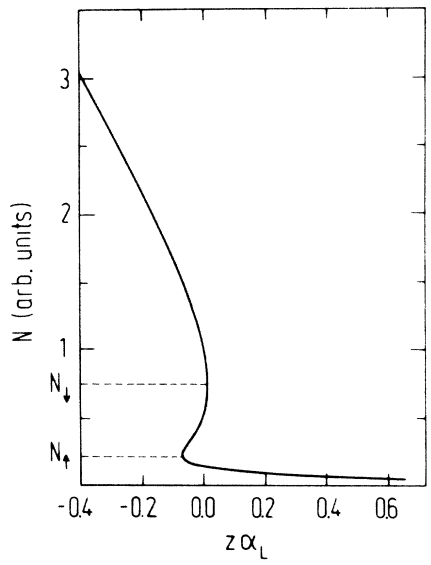

FIG. 3. Spatial variation of the density; stationary solution of Eq. (1) using the model absorption (Ref. 10) discussed in the text. The critical densities $N_\uparrow$ and $N_\downarrow$ correspond to the turning points of the curve, the part with positive slope is unstable.

some point in the crystal the intensity falls below $I_\downarrow$. Behind this point the steady-state solution follows the lower bistable branch. Somewhere in the crystal, where the intensity is between $I_\uparrow$ and $I_\downarrow$, there is a discontinuous jump, called a kink, in the density profile.

An integration of Eqs. (7) and (8) gives the integral

$$z = C - \frac{1}{\alpha(N)} - \int_{N_0}^{N} \frac{dx}{x\alpha(x)} \equiv C + f(N) . \tag{11}$$

The constant N_0 is arbitrary but fixed and the integration constant C is to be determined by the input intensity and the continuity of the intensity. When $f(N)$ is known, formula (11) can be locally inverted to yield

$$N(z) = f^{-1}(z - C) . \tag{12}$$

Hence, the constant C and thus the initial intensity I_0 only sets the origin of the curve but do not change its overall shape. The shape is exclusively determined by the properties of the absorption coefficient. A unique inversion of (12) is, however, not possible over the whole range of N since the function $f(N)$ is not monotonic in N. In Fig. 3 a model absorption[10] is used to plot the general features of $f(N)$.

The inversion must be made separately between the successive zeros of df/dN. By using (11) and (12) we obtain the condition for the zeros in the form

$$\frac{d}{dN}\left[\frac{N}{\alpha(N)}\right] = 0 . \tag{13}$$

Hence, the zeros equal the critical densities $N_\uparrow$ and $N_\downarrow$ (see Fig. 2). When $I(z)$ is solved from (7) and (11) it is also multivalued as a function of z. In Fig. 4 this is plotted for the model absorption.[10] It is clear that the mathematical solution (11) as such cannot describe the physically acceptable solution if the multivalued region lies inside the crystal. However, from the mathematical solution one obtains one physical solution by matching the intensities at the intersection point $z = \bar{z}$. This resembles the generalized Maxwell construction in the theory of first-order phase transitions. One may also obtain other stationary solutions of the differential equation (5), in which the point of discontinuity, i.e., the kink position, may be anywhere in the range of z in which the intensity varies between the critical values $I_\uparrow$ and $I_\downarrow$. In the thermodynamic sense one would characterize these solutions as metastable states. They are, however, important to understand the dynamical properties of the system, as will become clear in the following sections. The density branch between $N_\uparrow$ and $N_\downarrow$ (Fig. 3) is unstable and must be excluded from the physical steady-state solution. The solution in the front part of the crystal corresponds to the upper bistable branch. In the following, we will denote this part of the density profile as the "upper-branch solution," N_U, and the remainder as the "lower-branch solution," N_L, respectively. The upper branch solution is fixed by the boundary condition at the crystal front face ($z = 0$). The range of the possible positions of the density

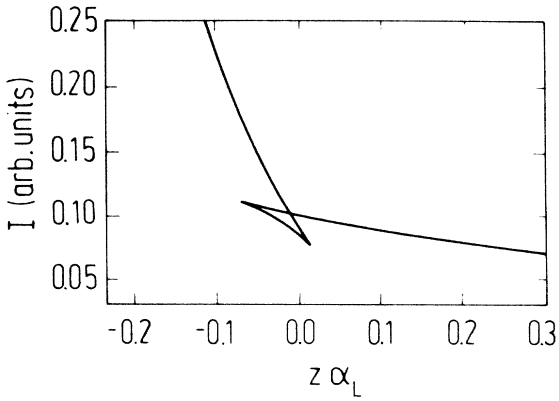

FIG. 4. Spatial profile of the intensity corresponding to the density shown in Fig. 3.

kink is bounded by the positions of the critical intensities $I_\uparrow$ and $I_\downarrow$ which are determined by the integrals

$$\ln(I_\downarrow/I_0)=-\int_0^{z_\downarrow}\alpha(N_U(z'))dz'$$

and (14)

$$\ln(I_\uparrow/I_0)=-\int_0^{z_\uparrow}\alpha(N_U(z'))dz' .$$

Since $I_\uparrow > I_\downarrow$ we have $z_\uparrow < z_\downarrow$. Equations (14) show that both $z_\uparrow$ and $z_\downarrow$ which bound z_c depend on the actual value of the input intensity, whereas the range $z_\downarrow - z_\uparrow$ does not. In general, the integration constant of the lower-branch solution is different from that of the upper-branch solution. The matching condition of the two branches at the kink position can be set in the form

$$\frac{N_U(z_c)}{\alpha(N_U(z_c))}=\frac{N_L(z_c)}{\alpha(N_L(z_c))} . \quad (15)$$

This is a direct consequence of the requirement that the intensity is continuous at $z=z_c$. In Fig. 5 we show a typical matched solution. A very important feature is that for $z_c > z_\uparrow$, the intensity immediately behind the kink is below the critical value $I_\uparrow$ for switchup. Consequently, the density is below $N_\uparrow$. This stabilizes the position of the kink.

To analyze this stability, we investigate the response of the density profile to a small change of the input intensity. Therefore, we assume that a kink has already been formed at the position z_c which is larger than $z_\uparrow$. Hence $I(z_c) < I_\uparrow$ and $N(z_c+\delta z) < N_\uparrow$. After this situation has been established, the intensity is suddenly increased to a value $\bar{I}_0$, which, however, is supposed to allow still a steady-state profile $I(z)$ with a value $I(z_c) < I_\uparrow$. In other words, the change of the input intensity is such that locally, at the kink position z_c, it does not exceed the bistable

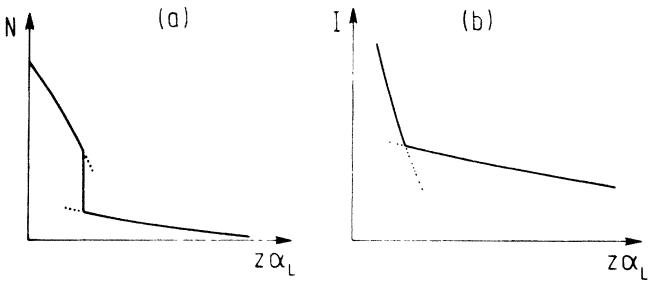

FIG. 5. (a) Kink structure in the density profile. This solution is obtained from the mathematical steady-state solution (Fig. 3) by choosing a kink position $z_c < z_\downarrow$. The density for $z < z_c$ follows the upper bistable branch. The profile for $z > z_c$ is obtained from the following two conditions. (i) $N < N_\uparrow$, i.e., the density in the region behind the kink follows the lower bistable branch. (ii) The intensity is continuous at $z=z_c$. These conditions restrict the possible values for z_c to a well-defined interval. (b) The intensity profile (matched solution) corresponding to $N(z)$ shown in (a).

regime. We will show that under these conditions the kink position remains fixed and the density distribution relaxes to a steady-state kink profile $\bar{N}(z)$ corresponding to the increased intensity $\bar{I}_0$. We denote the actual profile by $N(z,t)$ and investigate whether the difference

$$\delta N(z,t)=N(z,t)-\bar{N}(z)$$

tends to decrease or to increase with time. Because of the small change of the input intensity, we assume $\delta N(z,t)$ to be small; however, we do not assume $N(z,t)$ initially to be in any steady state. Rewriting Eq. (5) in terms of δN yields

$$\frac{\partial}{\partial t}\delta N(z,t)=\frac{\alpha(N(z,t))}{\hbar\omega}\bar{I}_0\exp\left[-\int_0^z\alpha(N(z',t))dz'\right]-\frac{\alpha(\bar{N}(z))}{\hbar\omega}\bar{I}_0\exp\left[-\int_0^z\alpha(\bar{N}(z'))dz'\right]-\frac{\delta N(z,t)}{\tau} . \quad (16)$$

We expand linearly to obtain

$$\frac{\partial}{\partial t}\delta N(z,t)\simeq-\lambda(z)\delta N(z,t) - \frac{\alpha(\bar{N})}{\hbar\omega}\bar{I}(z)\int_0^z\alpha'(\bar{N})\delta N(z',t)dz' , \quad (17)$$

where

$$\alpha'(\bar{N})=\left.\frac{\partial\alpha}{\partial N}\right|_{N=\bar{N}}$$

and

$$\lambda(z)=1/\tau-\frac{\alpha'(\bar{N})}{\hbar\omega}\bar{I}(z) .$$

$\lambda(z)$ is strictly positive because of the condition $I(z_c) < I_\uparrow$. We show in the Appendix that the solution of (17) decays to zero faster than

$$Me^{-\lambda_{\min}t}e^{2(Ptz)^{1/2}} ,$$

where $\lambda_{\min}$ is the minimum value of $\lambda(z)$ and M and P are constants defined in the Appendix.

Thus, $N(z,t)\to\bar{N}(z)$ for increasing times. This means that for sufficiently small changes of the input intensity the kink position stays fixed and the density varies locally according to the upper bistable branch for $z < z_c$ or according to the lower bistable branch for $z > z_c$, respectively. The kink starts to be formed at a new position only when it is no longer possible to have a kink at z_c or, equivalently, when $\bar{I}(z_c)$ becomes larger than $I_\uparrow$. This stability of the kink position largely influences the dynamical properties of the system.

IV. THE DYNAMICS OF THE KINK FORMATION

If the input intensity varies in time the steady-state description fails to explain the details of kink formation and the propagation process. The main reason is that the response time of the system to a change of the intensity is

of the order of the electron-hole-pair lifetime τ. Hence, if the intensity is changing continuously, the system cannot be in equilibrium with the instantaneous value of the intensity. For simplicity, we assume the input intensity to rise linearly

$$I_0(t)=\bar{I}t \ , \tag{18}$$

and the absorption coefficient to be nearly constant for the lower branch. Inserting these conditions into (7) and (5) we obtain

$$\frac{\partial}{\partial t}N(z,t)=\frac{\alpha(0)}{\hbar\omega}\bar{I}te^{-\alpha(0)z}-N(z,t)/\tau \tag{19}$$

and

$$I(z,t)=\bar{I}te^{-\alpha(0)z} \ . \tag{20}$$

As mentioned earlier, the intensity reacts without delay to the changes of both the input intensity and the density. When (19) is solved we find the density in the form

$$N(z,t)=\frac{\alpha(0)}{\hbar\omega}\tau\bar{I}e^{-\alpha(0)z}(t-\tau+\tau e^{-t/\tau}) \ . \tag{21}$$

After the transient time period we see that N at time t is in a "steady state" with the intensity at the time $t-\tau$,

$$N(z,t)=\frac{\alpha(0)\tau}{\hbar\omega}I(z,t-\tau) \quad \text{with } t\gg\tau \ . \tag{22}$$

Hence, when the intensity at the front end reaches the critical switchup value $N_\uparrow$, the density is still not critical. Consequently, the absorption is still low and therefore the critical intensity can be reached in a wide region with the extension Δz,

$$\Delta z=\frac{1}{\alpha(0)}\ln\left[1+\frac{\bar{I}\tau}{I_\uparrow}\right]\simeq\frac{1}{\alpha(0)}\frac{\bar{I}\tau}{I_\uparrow} \ , \tag{23}$$

before the system even starts to decrease the local intensity by increasing the density and thus the absorption.

If the rise time of the input intensity is much longer than the electron-hole-pair lifetime τ, we can take τ as an expansion parameter. Integrating (1) yields

$$N(z,t)=\int_0^t dt' e^{-t'/\tau}\frac{\alpha(N(z,t-t'))}{\hbar\omega}I(z,t-t') \ . \tag{24}$$

For $t\gg\tau$ we expand in τ and obtain

$$N(z,t)\simeq\frac{\alpha(N(z,t-\tau))}{\hbar\omega}I(z,t-\tau)\tau[1+O(\tau^2)] \ . \tag{25}$$

This equation is a generalization of the result (22). It is valid when α and I_0 are both slowly changing functions of their arguments.

We demonstrate that this analysis is already able to describe the essential features of the kink-formation process. Since we could not solve the dynamical problem with any physically realistic absorption coefficients, we employed numerical methods. To keep the following analysis as transparent as possible, we use a simple model absorption, which, however, contains all essential features. It consists of two absorption levels which are connected by a linear slope

$$\alpha(N)=\begin{cases}\alpha_L, & N<N_\uparrow \\ \alpha_L+\dfrac{\alpha_H-\alpha_L}{N_\downarrow-N_\uparrow}(N-N_\uparrow), & N_\uparrow<N<N_\downarrow \\ \alpha_H, & N_\downarrow<N \ .\end{cases} \tag{26}$$

The slope of the linearly increasing part of the absorption profile turns out to be important for the dynamics of the kink-propagation mechanism, as will be explained in Sec. IV B. Note, however, that because of the instability of the stationary solution corresponding to that linearly increasing part of $\alpha(N)$, it does not influence the steady state.

In the model under discussion, the parameters characterizing the dynamics are α_H/α_L and $N_\downarrow/N_\uparrow$. They are defined by fitting Eq. (26) to the microscopically calculated absorption plotted in Fig. 1. Mathematically, we see that the expression (26) does not allow bistability for too flat slopes of the intermediate section of $\alpha(N)$. One may define a critical slope, which separates bistability from monostability. It is given by

$$\frac{(\alpha_H/\alpha_L)-1}{N_\downarrow/N_\uparrow-1}=1$$

or

$$\frac{\alpha_H}{\alpha_L}=\frac{N_\downarrow}{N_\uparrow} \ . \tag{27}$$

Near this limit, i.e., for weak bistability, the approximate equation (25) can be used.

A. Numerical calculations for the model absorption coefficient

To gain insight into the dynamics of the kink formation in the regime where the process is fast, we numerically integrate Eqs. (1) and (2) using the absorption model (26). As a result, we plot in Fig. 6(a) the density profile for six evenly spaced times t_i. The scaled switchup density $N_\uparrow=1$ is reached at t_2. The difference between the respective profiles at t_1 and t_2 is so small that they are not resolved as different curves in Fig. 6(a). The complete scenario in Fig. 6 shows that the kink is actually not running into the crystal but the density is increasing over a certain spatial region. After the switching process has started, the density has increased to the critical value $N_\downarrow$ in a time which is considerably smaller than τ after $N_\uparrow$ has been reached. This observation will be utilized in our subsequent analytical analysis (Sec. IV B). Moreover, the place of the kink z_c is stabilized long before the complete profile has been established. The density just behind the kink first rises but then drops to a value below the one which was reached at this point before the kink formation started. In Fig. 6(b), the switchingup of an additional layer of the crystal is shown for the same parameters. The kink at the second position is formed almost as if the edge of the kink in the first position would serve as a stationary boundary. The stages of the kink formation in the second position are a repetition of the ones in the first position.

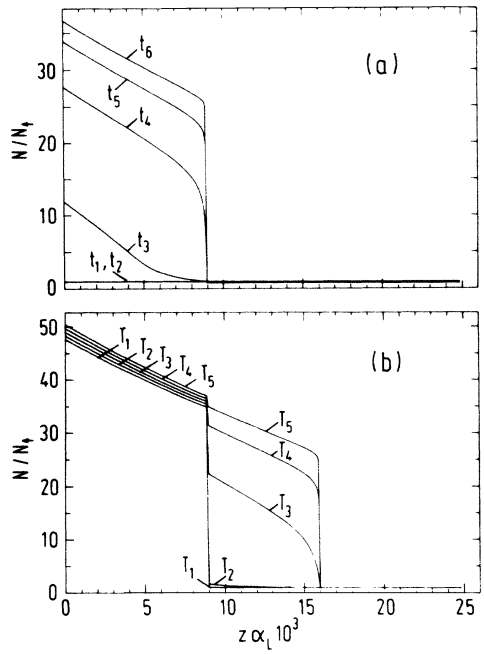

FIG. 6. (a) Formation of a density kink. The different curves correspond to the indicated time instants t_i, $t_{i+1}=t_i+\tau$. The parameters of the absorption, Eq. (26), are $\alpha_H/\alpha_L=35.0$ and $N_\downarrow/N_\uparrow=4.0$. The incident intensity is assumed to rise linearly according to $I_0(t)=I_\uparrow(t/50\tau)$. (b) Buildup of the density kink at the second position. The times are T_i, $T_{i+1}=T_i+\tau$.

In Fig. 7 we present the intensity profiles $I(z)$ which correspond to the density variations plotted in Fig. 6(a). One observes a sharp bending of $I(z)$ exactly at the position of the kink in $N(z)$. A comparison of Figs. 6(a) and 7 shows a drop of the local intensity in a large fraction of the crystal. This drop sets in immediately after the density begins to switchup ($t \gtrsim t_2$). For a sufficiently fast decrease of the intensity, the right-hand side of Eq. (1) becomes negative, causing also a decrease of the local density. Therefore, in the region behind the kink, the density drops even though it had already exceeded the switchup

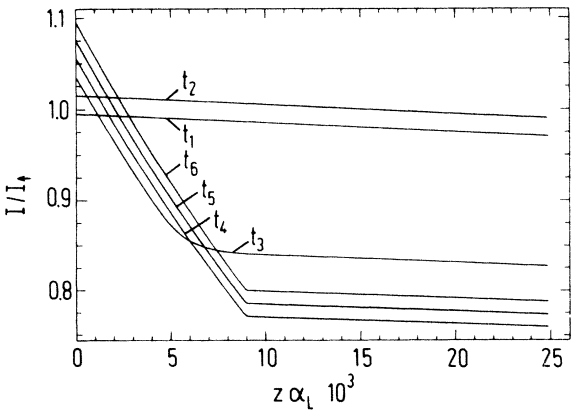

FIG. 7. Temporal development of the intensity profile corresponding to the formation of the density kink shown in Fig. 6(a). The times are the same as in Fig. 6(a).

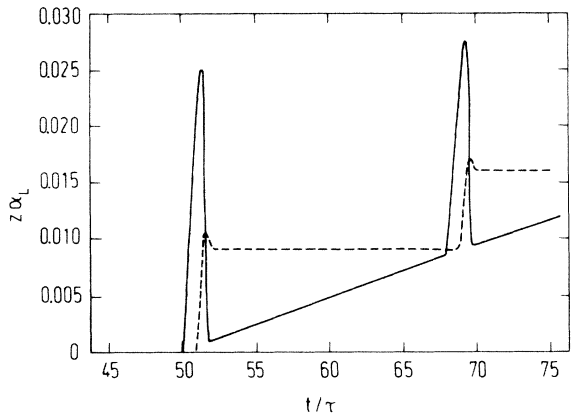

FIG. 8. Position of the critical intensity $I_\uparrow$ (solid line) and of the critical density $N_\uparrow$ (dashed line) as function of time for a linearly increasing incident intensity, $I_0(t)=I_\uparrow(t/50\tau)$. The parameters of the absorption coefficient, Eq. (26), are $\alpha_H/\alpha_L=35.0$ and $N_\downarrow/N_\uparrow=4.0$.

value $N_\uparrow$. This decrease of both the local density and the local intensity behind the kink leads to a stabilization of the kink position. In order for the kink to expand deeper into the crystal, the input intensity has to increase sufficiently so that the local intensity behind the kink position again reaches the switchup value $I_\uparrow$. This causes a pronounced delay and prevents a continuous kink movement.

This scenario is also shown in Fig. 8. Here, we plot as function of time the position where the intensity equals the critical switchup value $I_\uparrow$ together with the position where the density has the critical value $N_\uparrow$ (or changes from larger than $N_\uparrow$ to smaller than $N_\uparrow$ if a kink already exists). The delay between the curves shows that the system is not in a steady state. The peaks (shootover) to be seen in Fig. 8 before the stationary values are reached indicate that the system is unstable in a wider region than that which finally stays in the upper branch. A short moment of instability does not guarantee switching due to the finite response time of the density. A detailed investigation shows that the shootover of the position of the

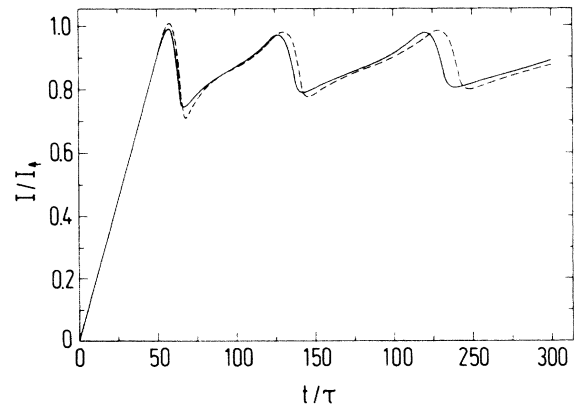

FIG. 9. Transmitted intensity as function of time for an incident intensity, $I_0(t)=I_\uparrow(t/50\tau)$. The numerical solution of Eqs. (1) and (4) is plotted as a solid line, the solution of (4) and the approximate Eq. (25) are shown as a dashed line.

switchup density $N_\uparrow$ becomes less pronounced for smaller ratios of the parameters $N_\downarrow/N_\uparrow$.

In Fig. 9 we compare the intensity transmitted through a crystal obtained from the approximation (25) with that determined by a numerical integration of the full Eqs. (1) and (4). We plot the transmitted intensity versus time for a linearly rising input intensity $I_0(t)=t/50$ (in the units of Fig. 9). A sawtooth structure in $I(t)$ is obtained, as already reported in Ref. 4(b) from a numerical analysis using the microscopic absorption coefficient for CdS. Each sawtooth corresponds to one cycle of the stepwise kink propagation. It can be seen that the analytical results obtained from Eq. (25) are in reasonable agreement with the solutions of the full transport equations. A drawback of the formula (25) is that one still has to perform a numerical iteration. However, its merits are that it exhibits the delay of the density explicitly.

B. Analytic estimates

Guided by the numerical results, we can obtain some simple analytic estimates for the kink properties. To keep the discussion as transparent as possible, we again use the idealized model absorption (26). First, we compute the kink position z_c. We denote by t_0 the time at which the intensity at the front face of the crystal reaches the switchup value,

$$I(z=0,t_0)=I_\uparrow \ .$$

The previous analysis has shown that it is a good approximation to assume the density to follow the intensity with a time delay τ,

$$N(z=0,t_1=t_0+\tau)=N_\uparrow \ .$$

The time interval t_2-t_1, which is needed to fix the place of the kink at z_c is approximated by the time in which the density at the front face of the crystal switches from $N_\uparrow$ to $N_\downarrow$,

$$N(z=0,t_2)=N_\downarrow \ .$$

This assumption is justified by the observation that once the absorption has locally reached the upper-branch value α_H, the intensity behind this region starts to decrease and the position of the switchup density $N_\uparrow$ cannot move deeper into the crystal (compare Fig. 8). Only the front part of the crystal $z<z_c$ becomes destabilized and switches to the upper bistable branch. Thus, the kink position z_c is determined through the condition that for $t=t_2$ the density at $z=z_c$ is just $N_\uparrow$,

$$N(z_c,t_2)=N_\uparrow=\alpha(N(z_c))\frac{\bar{I}\tau(t_2-\tau)}{\hbar\omega}e^{-\alpha_L z_c}$$
$$\simeq\alpha_L\frac{\bar{I}\tau(t_2-\tau)}{\hbar\omega}e^{-\alpha_L z_c} \ , \tag{28}$$

where Eqs. (18), (20), and (22) have been used. Approximating $\alpha(N)$ by α_L in (28) restricts our treatment to the situation in which the switching interval $t_2-t_1<\tau$. Eliminating $\bar{I}$ through the relation $\bar{I}t_0=I_\uparrow$ and using

$$N_\uparrow=\frac{\alpha_L I_\uparrow\tau}{\hbar\omega} \ ,$$

we obtain

$$z_c=\frac{1}{\alpha_L}\ln\left[\frac{t_2-\tau}{t_0}\right]\simeq\frac{1}{\alpha_L}\frac{t_2-\tau-t_0}{t_0}=\frac{1}{\alpha_L}\frac{t_2-t_1}{t_0} \ . \tag{29}$$

During the switching process, the absorption at the front face of the crystal ($z=0$) changes from $\alpha(z=0,t=t_1)=\alpha_L$ to $\alpha(z=0,t=t_2)=\alpha_H$ along the linearly increasing part (26)

$$\alpha=\alpha_L+\frac{\alpha_H-\alpha_L}{N_\downarrow-N_\uparrow}(N-N_\uparrow)=AN+B \ .$$

Using this relation, we can rewrite Eq. (1) at $z=0$

$$\frac{\partial\alpha}{\partial t}=\left[\frac{AI(z=0,t)}{\hbar\omega}-\frac{1}{\tau}\right]\alpha+\frac{B}{\tau} \ . \tag{30}$$

With $I(z=0,t)=I_0(t)=\bar{I}t$ and integrating (30) from t_1 to t_2, we obtain

$$\alpha_H=\alpha_L e^{a(\bar{t}_2^2-\bar{t}_1^2)}+\frac{B}{\tau}\int_{\bar{t}_1}^{\bar{t}_2}d\bar{t}\,e^{a(\bar{t}_2^2-\bar{t}^2)} \ , \tag{31}$$

where

$$\bar{t}_i=t_i-\frac{1}{2a\tau} \quad \text{and} \quad a=\frac{AI_\uparrow}{2\hbar\omega t_0} \ .$$

Approximating $\bar{t}^2-\bar{t}_i^2\simeq 2t_0(\bar{t}-\bar{t}_i)$, we can evaluate the integral in (31). The result for the switching interval is

$$t_2-t_1=\tau\frac{N_\downarrow/N_\uparrow-1}{\alpha_H/\alpha_L-1}\ln\left[\frac{(\alpha_H/\alpha_L-1)^2+N_\downarrow/N_\uparrow-1}{N_\downarrow/N_\uparrow-1}\right] \ . \tag{32}$$

Hence, t_2-t_1 is independent of t_0. Inserting (32) into (29) we see that

$$z_c\propto t_0^{-1} \ . \tag{33}$$

In Fig. 10, the numerical values of z_c are plotted versus α_H/α_L for $N_\downarrow/N_\uparrow=2.0$ and three different intensity rise times. For comparison, the values for the estimate (29) with (32) are also shown. One sees from Fig. 10 that the estimate is quite good for $\alpha_H/\alpha_L\gtrsim 10$. It breaks down for small ratios α_H/α_L, i.e., when the slope of the absorption (26) gets smaller. A systematic analysis shows that the approximate result overestimates the kink position if $N_\downarrow/N_\uparrow$ is increased. This failure can be readily understood since the increase of $N_\downarrow/N_\uparrow$ causes an increase of the rise time t_2-t_1 of the density, Eq. (32), hence opposing our original assumption that the switching time must be smaller than τ.

Besides the estimate for the kink position, it is also interesting to have an approximate relation between the time and distance of two successive kink-propagation steps. We assume, that at a given time the density profile exhibits a kink which is in a steady state with the momentary intensity. The kink at the new position deeper within the crystal starts to be formed when the local density

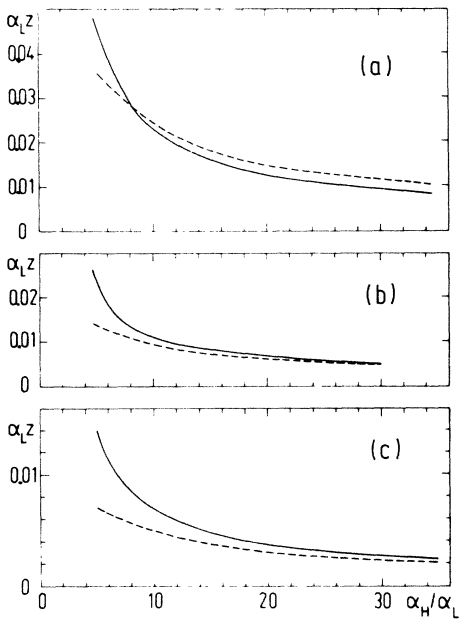

FIG. 10. Kink length as function of the absorption ratio α_H/α_L for a linearly rising incident intensity $I_0(t)=I_\uparrow(t/t_r)$. The other parameters are $N_\downarrow/N_\uparrow=2.0$ and (a) $t_r=20\tau$, (b) $t_r=50\tau$, (c) $t_r=100\tau$. The comparison is between the numerical result (solid lines) and the analytic approximation, Eq. (29) (dashed lines).

behind the existing kink reaches the switchup value, i.e., $N(z_i+\delta z)=N_\uparrow$. We denote by $N_{\uparrow U}$ the upper-branch value of the density corresponding to the switchup intensity $I_\uparrow$. This value is realized in the crystal at the position immediately before the kink

$$N(z_c-\delta z)=N_{\uparrow U} .$$

Using Eq. (11), we obtain

$$z_{c,n}=\frac{1}{\alpha[N(0)_n]}-\frac{1}{\alpha(N_{\uparrow U})}-\int_{N(0)_n}^{N_{\uparrow u}}dx\frac{1}{x\alpha(x)} ,$$

where $z_{c,n}$ is the position of the kink after the nth propagation and $N(0)_n$ is the density at the crystal front face ($z=0$) at the moment t_n when the kink starts to be formed at the $n+1$ position. The difference $z_{c,n+1}-z_{c,n}$ is given by

$$\begin{aligned} z_{c,n+1}-z_{c,n}&=\frac{1}{\alpha[N(0)_{n+1}]}-\frac{1}{\alpha[N(0)_n]} \\ &\quad+\int_{N(0)_n}^{N(0)_{n+1}}dx\frac{1}{x\alpha(x)} \\ &=\frac{1}{\alpha_H}\ln\left[\frac{N(0)_{n+1}}{N(0)_n}\right] , \end{aligned}$$

where we have used the model absorption (26). Using (22) and (18), we obtain

$$z_{c,n+1}-z_{c,n}=\frac{1}{\alpha_H}\ln\left[\frac{t_{n+1}-\tau}{t_n-\tau}\right]\simeq\frac{1}{\alpha_H}\frac{t_{n+1}-t_n}{t_n} ,$$

for $t_{n+1}-t_n\ll t_n$ and $t_n\gg\tau$. This relation again shows the direct connection of the kink propagation length $z_{c,n+1}-z_{c,n}$ with the duration of the switching process $t_{n+1}-t_n$.

V. SUMMARY

We presented a discussion of spatial and temporal aspects of the coexistence between regions of high and low excitation density in increasing-absorption optical bistability. The formation of a density kink is analyzed and the numerically observed stability of the kink position is investigated analytically. The propagation dynamics of the kink is shown to be a genuine dynamical property of the system which cannot be explained exclusively by the steady-state properties. Analytical approximations are obtained which are compared to the full numerical results. We find good agreement for the kink length and a simple estimate for the kink position.

ACKNOWLEDGMENTS

This work has been supported by the Commission of the European Community (under the experimental phase of the European Stimulation Action) and by the Deutsche Forschungsgemeinschaft through the Sonderforschungsbereich 65, Frankfurt/Darmstadt. One of the authors (S.W.K.) acknowledges financial support from the Deutsche Forschungsgemeinschaft.

APPENDIX

In this appendix we show some mathematical details of the proof that the solution of (17) approaches zero when time tends towards infinity. Inserting into (17)

$$\delta N(z,t)=\frac{N(z)}{\tau}e^{-\lambda(z)t}y(z,t) , \tag{A1}$$

we obtain for y the differential equation

$$\begin{aligned} \frac{\partial y(z,t)}{\partial t}&=-\int_0^z\alpha'(z')\frac{N(z')}{\tau} \\ &\quad\times e^{[\lambda(z)-\lambda(z')]t}y(z',t)dz' . \end{aligned} \tag{A2}$$

Imposing to (A2) the initial condition

$$y(z,t=0)=y_0(z) ,$$

we can integrate (A2) from zero to t. We obtain the Volterra-type integral equation

$$\begin{aligned} y(z,t)&=y_0(z)-\int_0^z\int_0^t\alpha'(z')\frac{N(z')}{\tau} \\ &\quad\times e^{[\lambda(z)-\lambda(z')]t'}y(z',t')dz'dt' . \end{aligned} \tag{A3}$$

We assume that the initial condition and the product

$$\alpha'(z)\frac{N(z)}{\tau}$$

are bounded. Hence,

$$|y_0(z)|\le Q \quad\text{and}\quad \left|\alpha'(z)\frac{N(z)}{\tau}\right|\le P , \tag{A4}$$

where Q and P are positive constants.

From the general theory of Volterra equations[11] it follows that the solution of (A3) is given in the form of a series

$$y(z,t)=\sum_{n=0}^{\infty} y^{(n)}(z,t) , \tag{A5}$$

which always converges for the type of kernel functions in our problem. The terms $y^{(n)}$ are calculated iteratively using the following procedure:

$$y^{(0)}(z,t)=y_0(z) ,$$
$$y^{(n+1)}(z,t)=-\int_0^z \int_0^t \alpha'(z')\frac{N(z')}{\tau} e^{[\lambda(z)-\lambda(z')]t'} \times y^{(n)}(z',t')dt'dz' . \tag{A6}$$

The solution (A1) can be estimated using (A5) and (A6). We show that

$$|y^{(n)}(z,t)| \le P^n Q e^{[\lambda(z)-\lambda_{\min}]t}\frac{(zt)^n}{(n!)^2} \quad \text{for } n\ge 1 .$$

For the proof of (A7) we use the method of complete induction. First, for $|y^{(1)}|$ we have

$$|y^{(1)}| \le \int_0^z \int_0^t \left|\alpha'(z')\frac{N(z')}{\tau}\right| e^{[\lambda(z)-\lambda(z')]t'} |y^{(0)}| dz'dt' \le PQ\int_0^z \int_0^t e^{[\lambda(z)-\lambda(z')]t'}dz'dt' \le PQe^{[\lambda(z)-\lambda_{\min}]t} zt . \tag{A7}$$

Hence, (A7) is true for $n=1$. Now, we assume it to be valid for n and obtain for $|y^{(n+1)}|$

$$|y^{(n+1)}| \le \int_0^z \int_0^t \left|\alpha'(z')\frac{N(z')}{\tau}\right| e^{[\lambda(z)-\lambda(z')]t'} |y^{(n)}| dz'dt' \le P^{n+1}Q\int_0^z \int_0^t e^{[\lambda(z)-\lambda(z')]t'} e^{[\lambda(z')-\lambda_{\min}]t'}\frac{z'^n}{n!}\frac{t'^n}{n!}dz'dt' \le P^{n+1}Qe^{[\lambda(z)-\lambda_{\min}]t}\frac{z^{n+1}}{(n+1)!}\frac{t^{n+1}}{(n+1)!} .$$

Thus, (A7) is true also for $n+1$ and subsequently for all $n\ge 1$. Using the result (A7) we obtain for $|\delta N(z,t)|$ the upper-bound estimate

$$|\delta N(z,t)| \le \frac{N(z)}{\tau}e^{-\lambda(z)t}|y(z,t)| \le \frac{N(z)}{\tau}e^{-\lambda(z)t}\sum_{n=0}^{\infty}|y^{(n)}| \le \frac{N(z)}{\tau}e^{-\lambda(z)t}Q\left[1+\left[\sum_{n=1}^{\infty}\frac{(Pzt)^n}{(n!)^2}\right]e^{[\lambda(z)-\lambda_{\min}]t}\right] . \tag{A8}$$

The sum on the right-hand side of (A8) is convergent and can be given in terms of the zeroth-order Bessel function with an imaginary argument $I_0(x)$. We obtain

$$|\delta N(z,t)| \le \frac{N(z)}{\tau}Q\{e^{-\lambda(z)t}+e^{-\lambda_{\min}t}[I_0(2\sqrt{Pzt})-1]\} . \tag{A9}$$

The asymptotic behavior of $I_0(x)$ is exponential,

$$I_0(x)\sim\frac{1}{\sqrt{x}}e^x \quad \text{when } x\to\infty . \tag{A10}$$

Inserting this, we obtain for large time periods

$$|\delta N(z,t)| \le Me^{-\lambda_{\min}t}e^{2\sqrt{Pzt}} ,$$

where M is a positive constant. Hence, when t tends towards infinity

$$|\delta N(z,t)| \to 0 .$$

[1]See, e.g., the *Proceedings of the Royal Society Discussion Meeting on Optical Bistability, Dynamical Nonlinearity and Photonic Logic* [Philos. Trans. R. Soc. London Ser. A **313** (1984)].

[2]For a discussion of the many-body theory of these effects, see H. Haug and S. Schmitt-Rink, Prog. Quantum Electron. **9**, 3 (1984).

[3]See, e.g., M. Dagenais and W. F. Sarfin, Appl. Phys. Lett. **45**, 210 (1984).

[4](a) H. E. Schmidt, H. Haug, and S. W. Koch, Appl. Phys. Lett. **44**, 787 (1984); (b) S. W. Koch, H. E. Schmidt, and H. Haug, *ibid.* **45**, 932 (1984); J. Lumin. **30**, 232 (1985).

[5](a) K. Bohnert, H. Kalt, and C. Klingshirn, Appl. Phys. Lett. **43**, 1088 (1983); (b) F. Henneberger and H. Rossmann, Phys. Status Solidi B **121**, 685 (1984).

[6]H. M. Gibbs, G. R. Olbright, N. Peyghambarian, H. E. Schmidt, S. W. Koch, and H. Haug, Phys. Rev. A **32**, 692 (1985).

[7]See, e.g., D. A. B. Miller, J. Opt. Soc. Am. **B1**, 857 (1984), for a discussion of some general aspects of increasing absorption optical bistability.

[8]S. W. Koch, *Dynamics of First-Order Phase Transitions in Equilibrium and Nonequilibrium Systems*, Vol. 207 of *Lecture Notes in Physics* (Springer, Berlin, 1984).

[9]H. Haug and S. W. Koch, IEEE Prog. Quantum Electron. (to be published).

[10]As model absorption we used the following:

$$\alpha(N)=A+B\frac{N^\beta}{1+CN^{2\beta}} ,$$

where A, B, C, and β are free, real, and positive variables. This function has the properties $\alpha(0)=A$ and $\alpha(\infty)=A$. It allows bistability when β is large enough. With this absorption model the integration in Eq. (11) can be made exactly.

[11]W. Pogorzelski, *Integral Equations and Their Applications* (Pergamon, New York, 1966), Vol. 1.